Transactions of the American Fisheries Society 139:900–910, 2010

DOI: 10.1577/T09-089.1

[Article]

Tail-Beat Patterns in Dual-Frequency Identification Sonar Echograms and their Potential Use for Species Identification and Bioenergetics Studies

ANNA-MARIA MUELLER*
Aquacoustics, Inc., Post Office Box 1473, Sterling, Alaska 99672, USA

DEBORAH L. BURWEN
Alaska Department of Fish and Game, 333 Raspberry Road, Anchorage, Alaska 99518, USA

KEVIN M. BOSWELL
Department of Oceanography and Coastal Sciences, Louisiana State University, Baton Rouge, Louisiana 70803, USA

TIM MULLIGAN
Department of Fisheries and Oceans, Pacific Biological Station, 3190 Hammond Bay Road, Nanaimo, British Columbia V9T 6N7, Canada

Abstract.—We observed patterns in echograms of data collected with a dual-frequency identification sonar (DIDSON) that were related to the tail beats of fish. These patterns reflect the size, shape, and swimming motion of the fish and also depend on the fish's angle relative to the axis of the beam. When the tail is large enough to reflect sound of sufficient intensity and the body is angled such that the tail beat produces periodic changes in the range extent covered by the fish image, then the tail beat becomes clearly visible on echograms that plot the intensity maximum of all beams. The analysis of DIDSON echograms of a mix of upstream-migrating Chinook salmon *Oncorhynchus tshawytscha* and sockeye salmon *O. nerka* resulted in the separation of two groups: (1) fish of sockeye salmon size that swam with a tail-beat frequency (TBF) between 2.0 and 3.5 beats/s and (2) fish of Chinook salmon size with a TBF between 1.0 and 2.0 beats/s. There was no correlation between TBF and fish size within each group, which suggests that the observed difference in TBF between the two groups was species-specific rather than an indirect effect of the groups' difference in size. The technique of extracting TBF from DIDSON echograms may also be useful for bioenergetics studies. Compared with electromyogram telemetry, it offers the advantages of being nonintrusive and faster to set up and analyze and therefore is suitable for analyzing larger sample sizes. The disadvantages are that the technique's potential is limited to relatively large fish, it can cover only relatively small areas, it cannot be used to follow individual fish over long distances, and some environments are too noisy to produce DIDSON images of sufficient quality.

Recent developments in sonar imaging have provided a means to acquire near-video-quality images of fish in waters that are too dark or turbid for traditional video techniques (Moursund et al. 2003; Mueller et al. 2006). Although originally developed for naval surveillance, the dual-frequency identification sonar (DIDSON; Sound Metrics Corp. [SMC], Lake Forest Park, Washington; Belcher et al. 2002) has been adopted by fishery scientists to obtain size and abundance estimates of fish (Moursund et al. 2003; Holmes et al. 2006; Burwen et al. 2007a; Boswell et al. 2008; Mueller et al. 2008), observe fish behavior relative to habitat and environmental stimuli (Tiffan et al. 2004; Xie et al. 2008), and study the effect of fish aspect angle on split-beam signals (Burwen et al. 2007b). Although DIDSON images show the approximate physical size and the general shape of the fish and thus provide more clues to identify fish species than are provided by traditional single-beam or split-beam sonars, species identification still remains one of the biggest challenges. Individual images allow confident identification only when the species present differ significantly in size or are unique in shape or swimming behavior (Burwen et al. 2007a; Mueller et al. 2008; D. L. Burwen, unpublished). Consequently, when multiple species are present, a netting or fish-wheel program is often run concurrently with the sonar program to apportion sonar counts to species (Westerman and Willette 2003; Brazil 2007; Miller et al.

* Corresponding author: am@aquacoustics.com

Received May 16, 2009; accepted December 30, 2009
Published online April 19, 2010

2007). Such programs can be costly, difficult to implement due to site constraints (McEwen 2006), and subject to selectivity biases that can become a major source of error (Carroll and McIntosh 2008; Fair et al. 2009).

Here, we explore whether DIDSON echograms capture fish tail-beat frequency (TBF) and other patterns in the swimming motion, with the idea that such patterns may help identify species. In steady-swimming mode, most fishes generate thrust with lateral movements of the body and caudal fin. Breder (1926) classified this type of locomotion into five broad categories, each characteristic of different species: anguilliform, subcarangiform, carangiform, thunniform, and ostraciiform. These swimming styles differ mainly in the amplitude of the lateral undulation and the fraction of the body that flexes.

In addition to potential species identification, the information on TBF contained in DIDSON echograms may also provide in situ estimates of energetic cost for bioenergetics studies. Tail-beat frequency has been widely used as a surrogate for energy consumption because several studies have demonstrated a close relationship between TBF and energy use (Brett 1995; Herskin and Steffensen 1998; Hinch and Rand 1998; Standen et al. 2002).

Methods

Data collection.—The salmon examples were taken from a mixture of upstream-migrating Chinook salmon *Oncorhynchus tshawytscha* and sockeye salmon *O. nerka* at an established acoustic-monitoring site located 14 km from the mouth of the Kenai River, Alaska (Miller et al. 2007). At this site, the river is approximately 100 m wide and is tidally influenced, with mid-channel water depth varying from 3 to 8 m. The site has a gradual and uniform bottom slope consisting mainly of mud and small gravel. The data were collected with a long-range DIDSON fitted with a high-resolution (large) lens in high-frequency mode (1.2 MHz). In this configuration, the images are built from 48 beams spaced 0.3° apart, which provide a 15° field of view horizontally and a 3° field of view vertically. Regardless of the configuration and sampled range, DIDSON images are always composed of 512 samples in range. The window length was set to 10 m, starting at a range of 13 m and ending at 23 m. The DIDSON system was deployed on a tripod-style stationary mount and was aimed across the river (toward the thalweg) perpendicular to the river flow. This configuration maximizes the potential for insonifying fish at side-aspect orientation as they swim through the acoustic beam. In practice, the fish often exhibit a swimming pattern that changes aspect orientation regularly (generally less than 45°) as they swim upstream. The data presented here were collected on July 22, 2007, during a period of neap tides, when the river current slowed down considerably at high tide but did not reverse.

The American eel *Anguilla rostrata* examples are downstream-migrating adults recorded in the intake canal of the Anson Hydroelectric Project on the Kennebec River, Maine (Mueller et al. 2008). The data were collected with the standard-version DIDSON in high-frequency mode (1.8 MHz), which builds the acoustic image from 96 beams spaced 0.3° apart and covering a 29° field of view horizontally and a 14° field of view vertically. The DIDSON system was deployed from a stationary pole mount and was aimed across the canal, with the wide axis of the transducer array (i.e., the 29° field of view) close to horizontal. The window length was set to 10 m, starting at a range of 5 m and ending at 15 m.

Data processing.—Background was removed from the images using the dynamic background-removal algorithm in SMC DIDSON Control and Display software (version 5.21). Display threshold and intensity were adjusted to optimize the contrast of the echo traces of interest. Echograms were generated in SMC DIDSON Control and Display software or in Echoview (version 4.60). Both software packages generate echograms suitable for visual review of tail-beat patterns; however, only Echoview exports frame time with the precision necessary (hundredths of a second) to calculate TBF.

Echograms are generated from DIDSON data by a process that collapses the individual range samples of each frame into a single column of data. The echogram thus consists of a series of columns representing a series of frames through time (Figure 1). We tested three types of echograms for the salmon examples. These preserved the range resolution of 512 samples but differed in the number of beams processed and the statistic used to summarize the sample intensity across beams as follows: (1) maximum intensity of all 48 beams, (2) maximum intensity of the 16 center beams, and (3) mean intensity of the 16 center beams. The echogram shown for the American eel examples is constructed from the maximum intensity of all 96 beams.

Fish length.—The manual fish-measuring tool included in SMC DIDSON Control and Display software was used to measure the length of the fish image. Display threshold and intensity settings were adjusted to optimize the contrast of the fish image. Efforts were made to take measurements only from frames where the fish appeared to display its full length and where the contrast between the fish image and

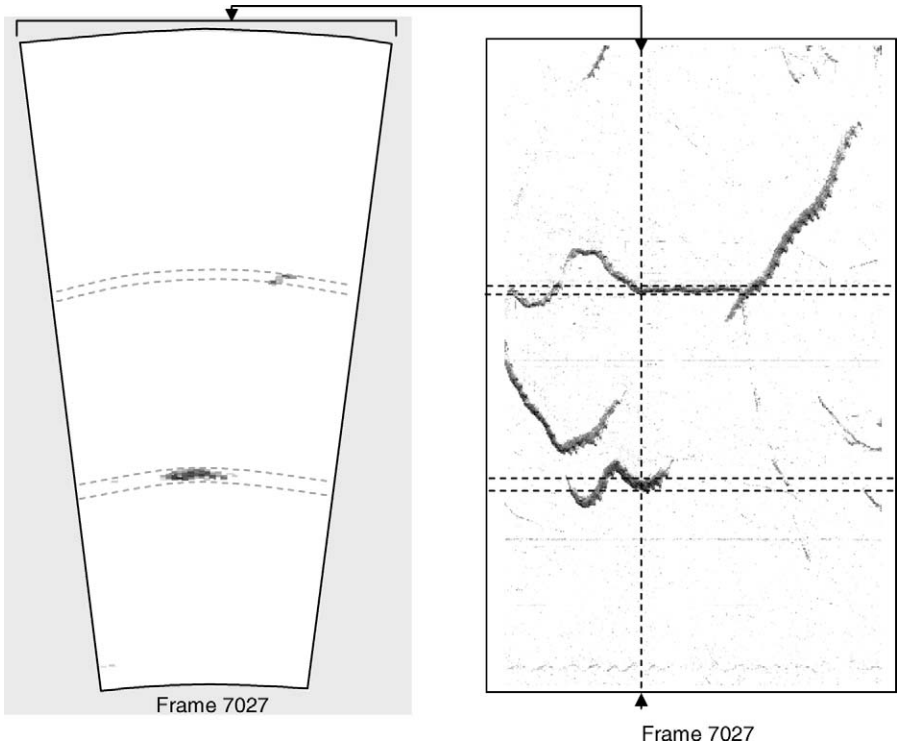

FIGURE 1.—Converting dual-frequency identification sonar (DIDSON) images to echograms. The image of each frame (left panel) is collapsed into one vertical column of data on the echogram (right panel). For each of the 512 range increments that make up the DIDSON image, a summary statistic is computed based on all or a subset of the beams. In the example shown, the image is built from an array of 48 beams. The echogram plots the maximum intensity of all 48 beams. The arcs (dashed line) on the image mark the same range interval that is marked by horizontal lines (dashed horizontal line) on the echogram. The dashed vertical line on the echogram indicates the frame corresponding to the image on the left. The range increases from the bottom to the top.

background was high. Each fish was measured on three different frames. The mean of these three measurements was used as an estimate of fish length.

Salmon species classification.—At the time of data collection in the Kenai River, there were two species of salmon present—Chinook salmon and the smaller but more numerous sockeye salmon. The species classification of DIDSON images was based on a combination of fish size and behavioral characteristics. Fish-wheel catch data indicate that for Kenai River sockeye salmon, the distribution of mid-eye-to-tail-fork lengths ends at a maximum of 70 cm (Tobias and Willette 2008), which converts to an estimated total length of 78 cm (D.L.B., unpublished data). Therefore, fish that produced DIDSON images that measured more than 80 cm in length were classified as Chinook salmon. Small Chinook salmon overlap in size with sockeye salmon. However, sockeye salmon have a greater tendency to travel in groups (Burgner 1991). Taking into account swimming behavior, fish images that measured 78 cm or less were classified as sockeye salmon. To reduce the ambiguity in the species classification, fish of intermediate size and solitary fish of sockeye salmon size were excluded from the data set.

Tail-beat frequency.—For each fish, we selected a period over which the 48-beam maximum echogram showed regular tail beats, clearly defined by the periodic extension of the tail to one side of the echo trace. We disregarded portions of the trace where the tail-beat pattern was ambiguous or where the fish trajectory changed direction in range. We used Echoview to mark each frame that produced a local peak in range and intensity in the echo trace of a given fish. We marked a minimum of four consecutive tail beats per fish. Using the time stamps (precision: hundredths of a second) of each selected frame, we calculated the TBF as follows:

$$\mathrm{TBF} = \frac{n-1}{\sum_{i=1}^{n-1}(t_{i+1} - t_i)},$$

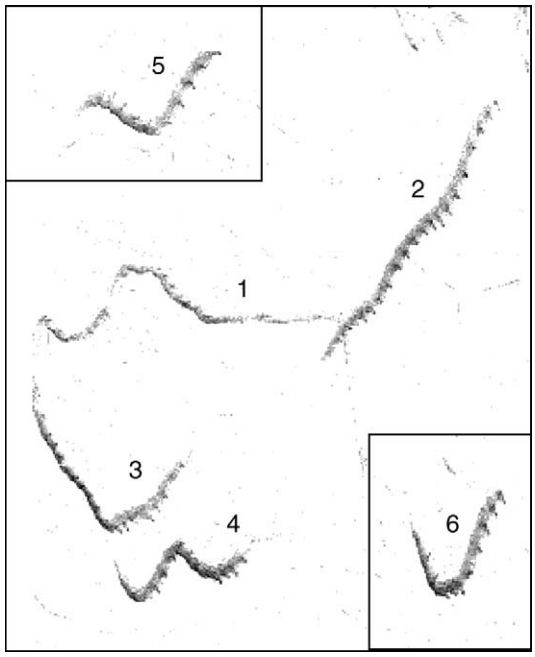

FIGURE 2.—A 48-beam maximum-intensity echogram of upstream-migrating salmon. The range increases from the bottom to the top, and time increases from left to right. Note the clearly visible "caterpillar legs" on traces that are angled towards or away from the transducer and their disappearance where trace 1 changes to horizontal (fish no longer changed in range). The part of the figure showing fish 1–4 is one contiguous section of the echogram. The boxes showing fish 5 and 6 are additional examples from different time periods inserted at the correct range.

where n is the number of successive local peaks examined and t_i is the time when peak i was recorded.

Statistical analysis.—The two-tailed Welch's t-test was used to compare the TBFs of salmon during a rising and a falling tide (Welch 1947). Welch's t-test is an adaptation of Student's t-test that does not assume equal variances for the two samples.

Results

Echograms of data collected with a side-looking DIDSON often show temporal patterns within the echo traces generated by fish swimming through the beam. For upstream-migrating salmon, these patterns resembled the shape of caterpillars with legs extending to one side (Figure 2). These patterns were obvious on echograms that were based on the intensity maximum over all 48 beams (Figure 3). When the number of beams used in the echogram is reduced to 16 (beams 16–32), the length of each echo trace and the number of "caterpillar legs" are reduced significantly. On echograms that use the mean intensity instead of the maximum, the trace blurs and the caterpillar leg pattern disappears.

Close examination of the data showed that the temporal patterns are created by periodic changes in the range extent covered by the fish image (Figures 4–6). A frame-by-frame comparison of the echogram and the corresponding images revealed that local peaks (i.e., caterpillar legs) are created when the tail of the fish increases the total range extent (Figures 5, 6; a DIDSON video clip of two upstream-migrating salmon can be viewed at www.aquacoustics.com/tail-beat-patterns.html). Each local peak coincided

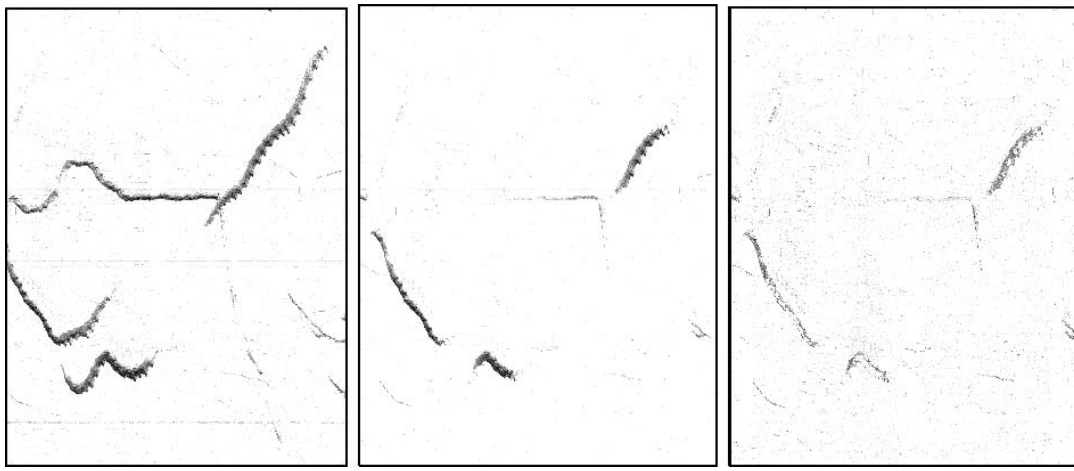

FIGURE 3.—Comparison of 48-beam maximum-intensity (left), 16-beam maximum-intensity (center), and 16-beam mean-intensity (right) echograms. Note the shortening of echo traces and the almost complete disappearance of one trace on the 16-beam echograms and the blurring on the 16-beam mean echogram. The range increases from the bottom to the top.

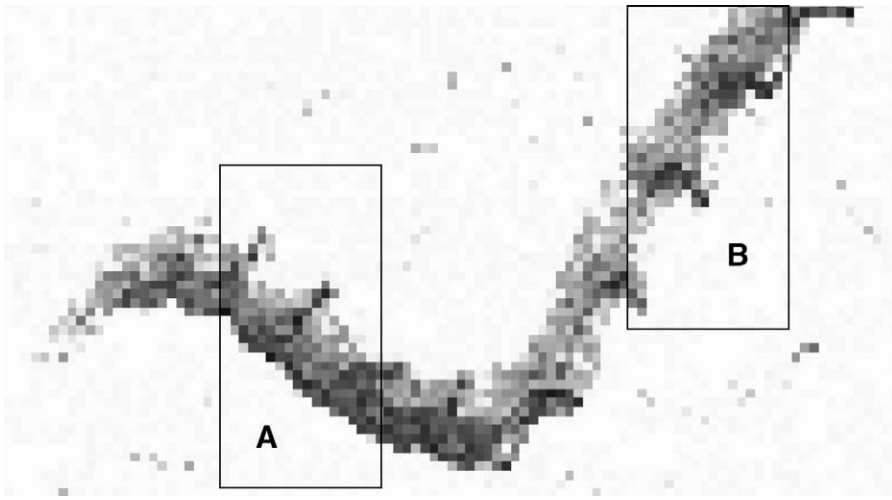

FIGURE 4.—Enlargement of a salmon echo trace (fish 5 in Figure 2). More detail for areas A and B is shown in Figures 5 and 6, respectively.

with a consistent position of the tail within the tail-beat cycle. The time interval between successive peaks is thus related to the TBF.

In the case of the salmon example data set, the tail was typically visible only on one side of the echo trace. Depending on the angle of the fish, the tail was only visible either on the near side or the far side of the trace (Figures 5, 6). Generally, the peaks were visible on the far side of the trace when the fish trajectory angled towards the transducer and were visible on the near

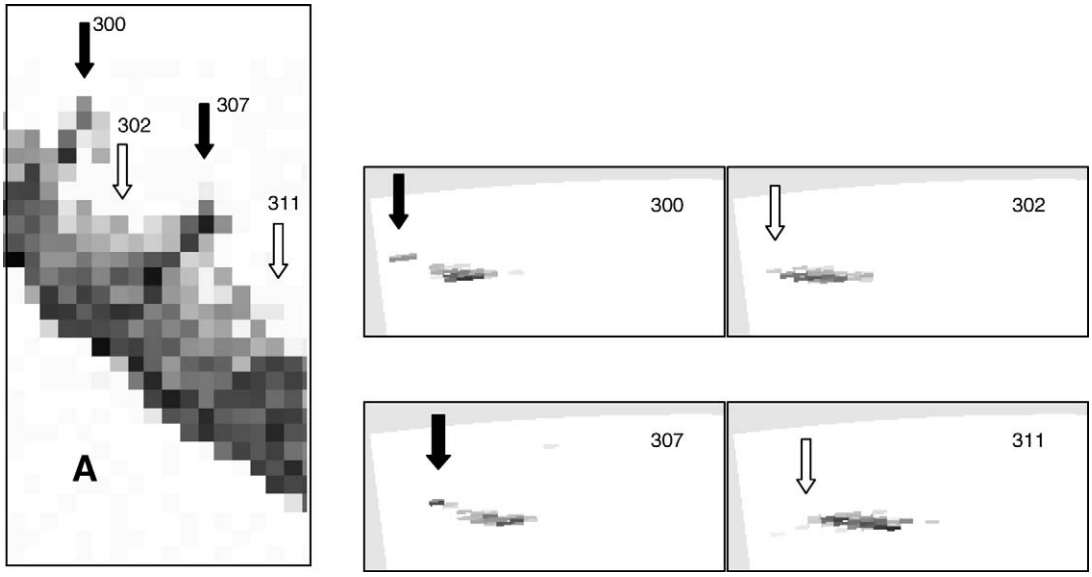

FIGURE 5.—Frame-by-frame examination of the dual-frequency identification sonar (DIDSON) echogram pattern when the trajectory of the fish is angled towards the transducer. The panel on the left is an enlarged section of the echogram shown in Figure 4. The four smaller panels show a section of the DIDSON image on the frames marked on the echogram. Black arrows indicate frames on which the fish image produced a local peak in the echo trace. White arrows indicate frames on which the fish image produced a local trough in the echo trace. The range increases from the bottom to the top. On frames 300 and 307, the tail is clearly visible and increases the total range extent covered by the fish image. The tail is visible at a range greater than the main body.

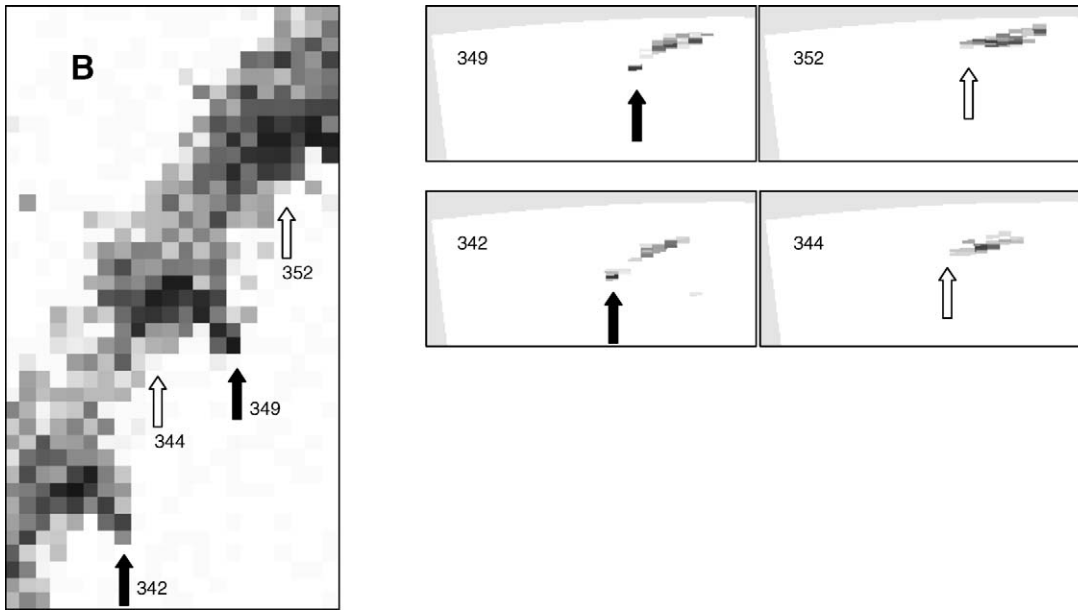

FIGURE 6.—Frame-by-frame examination of the dual-frequency identification sonar (DIDSON) echogram pattern when the trajectory of the fish is angled away from the transducer. The panel on the left is an enlarged section of the echogram shown in Figure 4. The four smaller panels show a section of the DIDSON image on the frames marked on the echogram. Black arrows indicate frames on which the fish image produced a local peak in the echo trace. White arrows indicate frames on which the fish image produced a local trough in the echo trace. The range increases from the bottom to the top. On frames 342 and 349, the tail is clearly visible and increases the total range extent covered by the fish image. The tail is visible at a range smaller than the main body.

side when the trajectory angled away from the transducer (Figure 2). The tail-beat peaks are more pronounced on large fish (e.g., fish 2–6 in Figure 2) than on small fish (e.g., fish 1 in Figure 2). When the trajectory of the fish runs parallel to the transducer, the echogram may not show a clear pattern of peaks and troughs. This is especially the case with smaller fish (e.g., fish 1 in Figure 2).

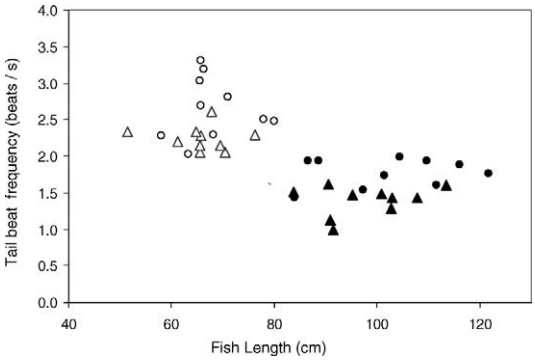

FIGURE 7.—Scatter plot of tail-beat frequency (beats/s) versus length of fish that were classified as sockeye salmon (open symbols) or Chinook salmon (black symbols) and that were detected during a rising tide (triangles) or falling tide (circles) in the Kenai River, Alaska.

When we measured fish lengths and TBFs of 40 salmon, we obtained the result shown in Figure 7. All fish that had been classified as Chinook salmon based on their lengths had TBFs less than 2 beats/s, while all actively migrating fish classified as sockeye salmon had TBFs greater than 2 beats/s. The difference between the two groups was statistically significant (two-tailed Welch's t-test: $P < 0.0001$, df = 34). For both species, data collected during the falling tide showed higher TBFs than data collected during the rising tide. This trend was statistically significant for both species (two-tailed Welch's t-test; Chinook salmon: $P < 0.001$, df = 17; sockeye salmon: $P < 0.015$, df = 11). The mean TBF of fish classified as Chinook salmon was 27% higher in the falling-tide sample than in the rising-tide sample, while for fish classified as sockeye salmon the difference in TBF was 18%.

As a second example, we examined images and echograms of adult out-migrating American eels. This data set illustrates the effect of body shape, swimming motion, aspect angle, and trajectory relative to the beam array. Figures 8–10 show three examples of the

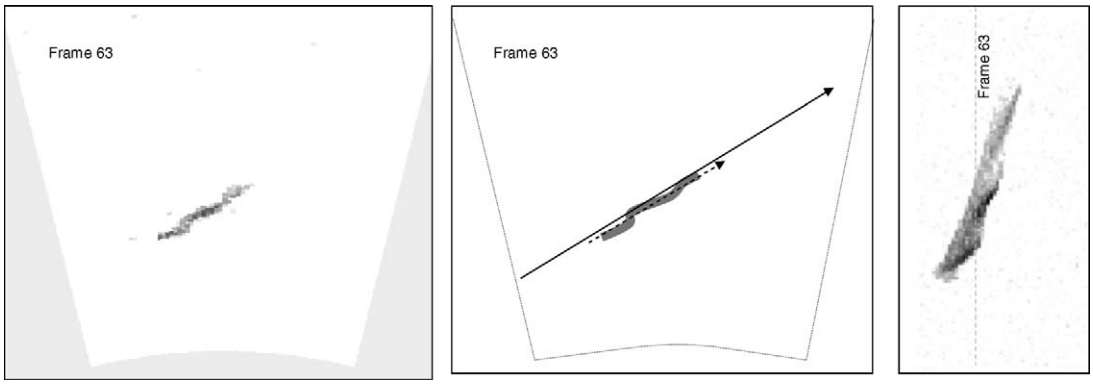

FIGURE 8.—American eel example 1: the eel image (left panel); a sketch (center panel) of the relative geometry between the beam, the eel's aspect angle, axis of sinusoidal motion (dashed arrow), and trajectory (solid arrow); and the corresponding echogram (right panel). The dashed vertical line on the echogram indicates the frame shown in the left and center panels. The eel's trajectory is oriented at an angle of approximately 60° relative to the acoustic axis of the center beam. The axis of the eel's sinusoidal motion is parallel to its trajectory.

patterns generated in the echogram. The echo traces of American eels 1 and 3 resembled the shape of a saw blade, while the echo trace of American eel 2 formed a strikingly different herringbone pattern (corresponding DIDSON video clips can be viewed at www.aquacoustics.com/tail-beat-patterns.html). Of the 57 eels we examined, most created echogram patterns similar to those of American eels 1 and 3. Compared with the caterpillar shapes of the salmon examples (Figure 2), the local peaks in the American eel traces are angled more in the direction of the eel's trajectory on the echogram. Frame-by-frame examination of the source images in video mode indicated that as the American eel's body undulates from side to side, it forms a series of alternating convex and concave regions that are separated in range. This type of swimming motion translates into an echogram pattern composed of multiple parallel streaks over time.

The form of the pattern also depends on the geometric relationship between the DIDSON beam, the fish, and the fish's trajectory (Figures 8–10). The striking herringbone pattern shown in the echogram panel of Figure 9 was created by an American eel that was oriented roughly parallel to the acoustic axis of the center beam. As this individual was drifting across the beam, it was undulating continuously from side to side. Its trajectory barely changed in range. Although American eel 2 is the same type of fish and of similar size as American eels 1 and 3, its echogram pattern differs dramatically because of the different geometry

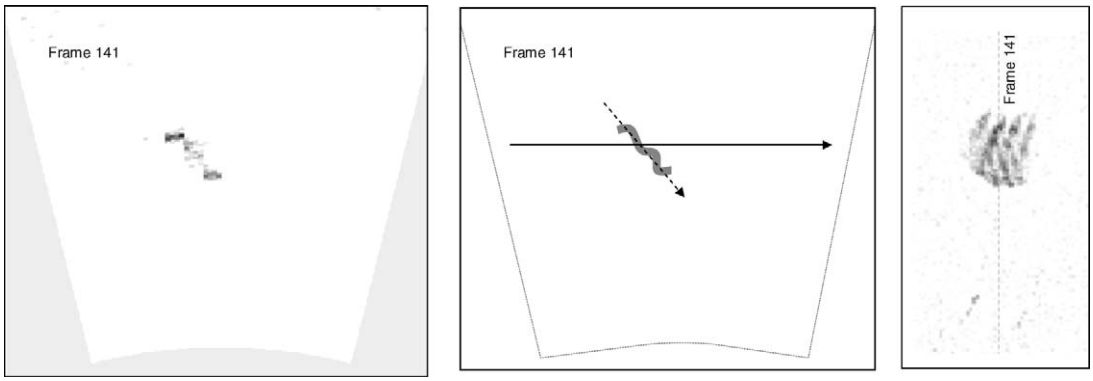

FIGURE 9.—American eel example 2: the eel image (left panel); a sketch (center panel) of the relative geometry between the beam, the eel's aspect angle, axis of sinusoidal motion (dashed arrow), and trajectory (solid arrow); and the corresponding echogram (right panel). The dashed vertical line on the echogram indicates the frame shown in the left and center panels. The eel's trajectory is oriented perpendicular to the acoustic axis of the center beam. The axis of the eel's sinusoidal motion encloses an angle of approximately 45° with its trajectory.

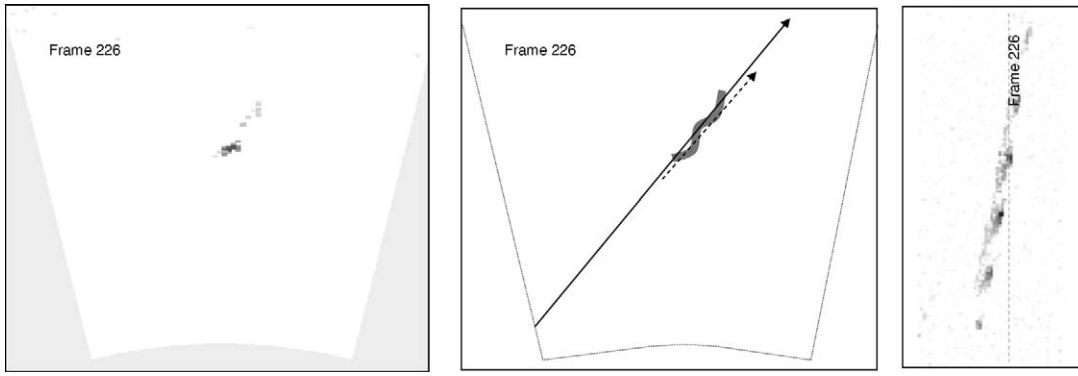

FIGURE 10.—American eel example 3: the eel image (left panel); a sketch (center panel) of the relative geometry between the beam, the eel's aspect angle, axis of sinusoidal motion (dashed arrow), and trajectory (solid arrow); and the corresponding echogram (right panel). The dashed vertical line on the echogram indicates the frame shown in the left and center panels. The eel's trajectory is oriented at an angle of approximately 40° relative to the acoustic axis of the center beam. The axis of the eel's sinusoidal motion is parallel to its trajectory.

involved. The trajectories of American eels 1 and 3 are roughly parallel to the axis of their bodies' sinusoidal motion (Figures 8, 10), whereas in the case of American eel 2 the trajectory and the axis of sinusoidal motion enclose an angle of approximately 45° (Figure 9).

The echogram patterns of American eels 1 and 3 are more similar to each other than to that of American eel 2, with the main difference being that the trace of eel 1 appears more solid compared with that of eel 3. This can be explained partly by American eel 1 being larger, at least when measured on the DIDSON image, but the more important factor in this case is the aspect angle. The body of American eel 1 forms an angle of approximately 45° with the acoustic axis of the center beam, while American eel 3 is oriented at a noticeably more oblique angle. As a consequence, American eel 1 reflects a strong signal along most of its body. By contrast, American eel 3 reflects a strong signal only along parts of the body. The shifting location of strong and weak signals along its body coincides with its sinusoidal movement. Because only part of its body produces a strong signal at any given moment, the resulting echogram pattern of American eel 3 appears less solid than that of American eel 1.

Discussion

The relationship between the salmon echogram pattern and the tail-beat cycle was confirmed by careful frame-by-frame examination of the corresponding images in video mode, which shows that the periodic appearance of the tail is consistent with the changes in the body curvature that accompany each tail-beat cycle. When the fish tail is large enough to reflect sound of sufficient intensity and when the body is angled such that the tail beat produces periodic changes in the range extent covered by the fish image, then the tail beat becomes clearly visible on DIDSON echograms that plot the maximum intensity of all beams.

One important factor that determines whether DIDSON echograms can be used to derive TBF is the frame rate at which the data have been collected. The frame rate needs to be more than twice the TBF; if the frame rate is lower, then the true pattern will be distorted by aliasing (Shannon 1949; Harris 2006). A good illustration of this fundamental sampling principle can be seen at www.dsptutor.freeuk.com/aliasing/AD102.html. As an extreme example, if the TBF and the frame rate are the same, no tail movement would be apparent because in each frame the tail would be observed at the same position relative to the body. The maximum frame rate that can be achieved depends on the maximum range sampled, the number of pings required to build a frame, and the computer and network configuration (B. Hanot, SMC, personal communications). In the case of the salmon data set, the maximum range sampled (23 m) limited the mean frame rate to 7.7 frames/s. The highest TBF that can be represented at this frame rate without aliasing is 3.8 beats/s.

The development of DIDSON has led to improved estimates of the physical size and, to some extent, the shape of the fish. If the species of interest are large enough to produce good DIDSON images and are of unique size, shape, or behavior, it is possible to determine species based on the image (Mueller et al. 2008). However, this is often not the case. For example, Kenai River Chinook salmon and sockeye

salmon are similar in shape and have some overlap in size (Burwen et al. 2003).

We found that TBF has potential for discriminating between sockeye salmon and Chinook salmon migrating upstream at a given site. Analysis of the TBFs of a mix of Chinook salmon and sockeye salmon resulted in the separation of two groups: (1) fish of sockeye salmon size that swam with TBFs between 2.0 and 3.5 beats/s and (2) fish of Chinook salmon size with TBFs between 1.0 and 2.0 beats/s. It is important to note that the TBF analysis is independent of the length- and behavior-based species classification. Specifically, length and behavior do not enter into the calculation of TBF. The key result is that within each group, there is no correlation between TBF and fish size. Aside from size, there is only one obvious difference between the two groups: the probability of belonging to one species or the other. Therefore, the results suggest that the observed difference in TBF between fish of Chinook salmon size and those of sockeye salmon size is species-specific rather than an indirect effect of the two groups' difference in size. In other words, if the difference in TBF is not explained by size, then species specificity becomes the most plausible explanation. This conclusion could be strengthened further by collecting video data of mixed species in steady-swimming mode.

This difference in TBF was true for the entire test data set, despite the considerable difference in the current that the salmon experienced in the rising and falling tides. However, a larger data set collected over a wider variety of conditions should be examined to assess the full range of in situ variation in TBFs. If species-specific differences are greater than the variation introduced by changes in the environmental conditions over the period and area sampled, then TBF may provide a powerful clue for distinguishing Chinook salmon and sockeye salmon migrating upstream in steady-swimming mode.

Differences in TBF have also been reported for other Pacific salmon species. Sockeye salmon were shown to have lower TBFs at a given speed than pink salmon *O. gorbuscha* (Brett 1982; Williams and Brett 1987). Differences can also be found when comparing data from Averett (1969) for coho salmon *O. kisutch* and from Webb (1975, cited by Webb 1995) for sockeye salmon. Webb (1995) cited data for jack mackerel *Trachurus symmetricus* and several other species from Hunter and Zweifel (1971) and his own data (Webb 1982, 1984) when he suggested a general pattern of more-thunniform, solitary species having lower TBFs over most of their speed range than less-thunniform species.

Acoustic data collected with DIDSON provide spatial information in two dimensions: range and angular position with respect to the center beam of the array. Depending on the orientation of the beam array relative to the fish trajectory, DIDSON data can be used to calculate fish speed over ground (Mueller et al. 2008); also, when used in conjunction with TBF, these data can be used to calculate stride length (i.e., distance traveled per tail beat) over ground. When we examined the salmon data collected on the rising tide, we found a strong correlation between stride length and the physical length of the fish (data not shown). Stride length would thus not add much to the species discrimination power of length alone, at least not for the given data set. However, stride length through water may allow discrimination between other combinations of species as Videler (1993) described how stride length depends on the body shape and swimming style of a fish and therefore varies among species. To derive stride length through water, one needs to convert speed over ground to speed through water. This, in turn, requires information on the water velocity at the location of the fish.

The ability to distinguish species based on TBF would have several advantages over other methods used to apportion sonar counts. Net- and fish-wheel-apportionment programs are generally labor intensive and gear intensive. On the Kenai River, gill nets of two different mesh sizes are drifted for 8 h/d to obtain length frequency information used in a mixture model that apportions species based on length-related parameters from a split-beam sonar (Miller et al. 2007). Aside from the considerable amount of labor involved, the program also creates tension with local sport fishers who are displaced by the netting program. Another challenge for netting programs involves site constraints. McEwen (2006) discontinued the net-apportionment program on the Aniak River, Alaska, after 2 years because the nets could not be drifted through the area of highest fish passage due to submerged debris and risk of damage to the sonar equipment. Fish wheels are often the only alternative to netting programs, but they are prone to selectivity biases. Fair et al. (2009) noted that species selectivity by fish wheels is probably a major source of error in the estimation of sockeye salmon abundance at a sonar site on the Yentna River, Alaska. Finally, using acoustic information such as TBF would have the advantage of being noninvasive, which is an important consideration when studying rare or endangered species.

The appearance of the tail-beat pattern (i.e., the shape of the echo trace) not only contains information on TBF but also reflects the type of swimming style, which may provide further clues for species identification. The anguilliform swimming style of the

American eels formed echo traces that looked noticeably different from those produced by the subcarangiform salmon. However, the shape of the echo trace must be interpreted with caution. As the American eel examples illustrated, the echo trace is not only a function of body shape and swimming motion but is equally a function of the relative geometry between the transducer, the fish, and the fish's trajectory.

Aside from possible improvements in species identification, the ability to extract TBF from DIDSON data could also be used for bioenergetics studies because the TBF of fish in steady-swimming mode correlates closely with swim speed and oxygen consumption (Bainbridge 1958; Hunter and Zweifel 1971; Brett 1995; Herskin and Steffensen 1998). Independent of any species-specific difference in TBFs, we found the TBF of upstream-migrating salmon in our data set to be higher during the falling tide than during the rising tide. This result is consistent with the assumption that fish swimming against a stronger current have to work harder to make headway than fish that benefit from the incoming tide, which reduces the river current.

To date, efforts to estimate in situ TBF have relied on labor-intensive videographic data collection and analysis (Krohn and Boisclair 1994) or electromyogram (EMG) radiotelemetry (Hinch and Rand 1998; Standen et al. 2002; Brown et al. 2006). The former requires clear water, while the latter requires the surgical implantation of EMG transmitters and electrodes in addition to laboratory calibration of the relationship between the EMG pulse interval and TBF or swim speed. Extraction of TBF information from DIDSON echograms may prove to be a valuable alternative in some situations. This technique offers the advantages of being nonintrusive and requiring less time for setup and data analysis; thus, it is suitable for analyzing larger sample sizes. However, the technique's potential is limited to relatively large fish as previously discussed. The technique can cover only relatively small areas and cannot be used to follow individual fish over long distances. Also, some environments (e.g., the tailrace area below dams) are too noisy to produce DIDSON images of sufficient quality.

We conclude that under the right circumstances, the careful analysis of tail-beat patterns in DIDSON echograms promises to become a useful tool for improved species identification and bioenergetics studies.

Acknowledgments

This investigation was partially financed by the Federal Aid in Sport fish Restoration Act and by resident and nonresident recreational anglers fishing in Alaska. We thank Bill Nagy (U.S. Army Corps of Engineers), Joe Hightower (North Carolina Cooperative Fish and Wildlife Research Unit), Dan Rawding (Washington Department of Fish and Wildlife), and Don Degan (Aquacoustics, Inc.) for valuable comments on the manuscript.

References

Averett, R. C. 1969. Influence of temperature on energy and material utilization by juvenile coho salmon. Doctoral dissertation. Oregon State University, Corvallis.

Bainbridge, R. 1958. The speed of swimming of fish as related to size and to the frequency and amplitude of the tail beat. Journal of Experimental Biology 35:109–133.

Belcher, E. O., W. Hanot, and J. Burch. 2002. Object identification with acoustic lenses. Pages 187–192 *in* R. Werner, editor. Proceedings of the 2002 International Symposium on Underwater Technology. Institute of Electrical and Electronic Engineers, Piscataway, New Jersey.

Boswell, K. M., M. P. Wilson, and J. H. Cowan. 2008. A semiautomated approach to estimating fish size, abundance, and behavior from dual-frequency identification sonar (DIDSON) data. North American Journal of Fisheries Management 28:799–807.

Brazil, C. E. 2007. Sonar enumeration of Pacific salmon into the Nushagak River, 2003. Alaska Department of Fish and Game, Divisions of Sport Fish and Commercial Fisheries, Fishery Data Series 07-37, Anchorage.

Breder, C. M. 1926. The locomotion of fishes. Zoologica 4:159–256.

Brett, J. R. 1982. The swimming speed of adult pink salmon, *Oncorhynchus gorbuscha*, at 20°C and a comparison with sockeye salmon, *O. nerka*. Canadian Technical Report of Fisheries and Aquatic Sciences 1143.

Brett, J. R. 1995. Energetics. Pages 3–68 *in* C. Groot, L. Margolis, and W. C. Clarke, editors. Physiological ecology of Pacific salmon. University of British Columbia Press, Vancouver.

Brown, R. S., D. R. Geist, and M. G. Mesa. 2006. Use of electromyogram telemetry to assess swimming activity of adult spring Chinook salmon migrating past a Columbia River dam. Transactions of the American Fisheries Society 135:281–287.

Burgner, R. L. 1991. Life history of sockeye salmon (*Oncorhynchus nerka*). Pages 3–117 *in* C. Groot and L. Margolis, editors. Pacific salmon life histories. University of British Columbia Press, Vancouver.

Burwen, D. L., S. J. Fleischman, and J. D. Miller. 2007a. Evaluation of a dual-frequency imaging sonar for detecting and estimating the size of migrating salmon. Alaska Department of Fish and Game, Divisions of Sport Fish and Commercial Fisheries, Fishery Data Series 07-44, Anchorage.

Burwen, D. L., S. J. Fleischman, J. D. Miller, and M. E. Jensen. 2003. Time-based signal characteristics as predictors of fish size for a side-looking hydroacoustic application in a river. ICES Journal of Marine Science 60:662–668.

Burwen, D. L., P. A. Nealson, S. J. Fleischman, T. J.

Mulligan, and J. K. Horne. 2007b. The complexity of narrowband envelopes as a function of side aspect angle. ICES Journal Marine Sciences 64:1066–1074.

Carroll, H. C., and B. C. McIntosh. 2008. Sonar estimation of salmon passage in the Yukon River near Pilot Station, 2006. Alaska Department of Fish and Game, Divisions of Sport Fish and Commercial Fisheries, Fishery Data Series 08-65, Anchorage.

Fair, L. F., T. M. Willette, and J. W. Erickson. 2009. Escapement goal review for Susitna River sockeye salmon, 2009. Alaska Department of Fish and Game, Divisions of Sport Fish and Commercial Fisheries, Fishery Manuscript Series 09-01, Anchorage.

Harris, F. J. 2006. Multirate signal processing for communication systems. Prentice Hall, Upper Saddle River, New Jersey.

Herskin, J., and J. F. Steffensen. 1998. Energy savings in sea bass swimming in a school: measurements of tail beat frequency and oxygen consumption at different swimming speeds. Journal of Fish Biology 53:366–376.

Hinch, S. G., and P. S. Rand. 1998. Swim speeds and energy use of upriver-migrating sockeye salmon (*Oncorhynchus nerka*): role of local environment and fish characteristics. Canadian Journal of Fisheries and Aquatic Sciences 55:1821–1831.

Holmes, J. A., G. M. Cronkite, H. J. Enzenhofer, and T. J. Mulligan. 2006. Accuracy and precision of fish-count data from a "dual-frequency indentification sonar" (DIDSON) imaging system. ICES Journal of Marine Science 63:543–555.

Hunter, J. R., and J. R. Zweifel. 1971. Swimming speed, tail beat frequency, tail beat amplitude and size in jack mackerel, *Trachurus symmetricus*, and other fishes. U.S. National Marine Fisheries Service Fishery Bulletin 69:253–66.

Krohn, M. M., and D. Boisclair. 1994. Use of a stereo-video system to estimate the energy expenditure of free-swimming fish. Canadian Journal of Fisheries and Aquatic Sciences 51:1119–1127.

McEwen, M. S. 2006. Sonar estimation of chum salmon passage in the Aniak River, 2002. Alaska Department of Fish and Game, Divisions of Sport Fish and Commercial Fisheries, Fishery Data Series 06-33, Anchorage.

Miller, J. D., D. L. Burwen, and S. J. Fleischman. 2007. Estimates of Chinook salmon abundance in the Kenai River using split-beam sonar, 2005. Alaska Department of Fish and Game, Fishery Data Series 07-92, Anchorage.

Moursund, R. A., T. J. Carlson, and R. D. Peters. 2003. A fisheries application of a dual-frequency identification sonar acoustic camera. ICES Journal of Marine Science 60:678–683.

Mueller, A. M., T. Mulligan, and P. K. Withler. 2008. Classifying sonar images: can a computer-driven process identify eels? North American Journal of Fisheries Management 28:1876–1886.

Mueller, R. P., R. S. Brown, H. Hop, and L. Moulton. 2006. Video and acoustic camera techniques for studying fish under ice: a review and comparison. Reviews in Fish Biology and Fisheries 16:213–226.

Shannon, C. E. 1949. Communication in the presence of noise. Proceedings of the Institute of Radio Engineers 37:10–21.

Standen, E. M., S. G. Hinch, M. C. Healy, and A. P. Farrell. 2002. Energetic costs of migration through the Fraser River Canyon, British Columbia, in adult pink (*Oncorhynchus gorbuscha*) and sockeye (*Oncorhynchus nerka*) salmon as assessed by EMG telemetry. Canadian Journal of Fisheries and Aquatic Sciences 59:1809–1818.

Tiffan, K. F., D. W. Rondorf, and J. J. Skalicky. 2004. Imaging fall Chinook salmon redds in the Columbia River with dual-frequency identification sonar. North American Journal of Fisheries Management 24:1421–1426.

Tobias, T. M., and T. M. Willette. 2008. Abundance, age, sex and size of Chinook, sockeye, coho and chum salmon returning to Upper Cook Inlet, Alaska, 2007. Alaska Department of Fish and Game, Fishery Data Series 08-40, Anchorage. Available: sf.adfg.state.ak.us/FedAidPDFs/fds08-40.pdf. (March 2009).

Videler, J. J. 1993. Fish swimming. Chapman and Hall, London, UK.

Webb, P. W. 1975. Hydrodynamics and energetics of fish propulsion. Bulletin of the Fisheries Research Board of Canada 190:1–159.

Webb, P. W. 1982. Locomotor patterns in the evolution of actinopterygian fishes. American Zoologist 22:329–342.

Webb, P. W. 1984. Body form, locomotion and foraging in aquatic animals. American Zoologist 24:107–120.

Webb, P. W. 1995. Locomotion. Pages 71–99 *in* C. Groot, L. Margolis, and W. C. Clarke, editors. Physiological ecology of Pacific salmon. University of British Columbia Press, Vancouver.

Welch, B. L. 1947. The generalization of student's problem when several different population variances are involved. Biometrika 34:28–35.

Westerman, D. L., and T. M. Willette. 2003. Upper Cook Inlet salmon escapement studies, 2002. Alaska Department of Fish and Game, Commercial Fisheries Division, Regional Information Report 2A03-24, Anchorage.

Williams, I. V., and J. R. Brett. 1987. Critical swimming speed of Fraser and Thompson river pink salmon (*Oncorhynchus gorbuscha*). Canadian Journal of Fisheries and Aquatic Sciences 44:348–356.

Xie, Y., C. G. Michielsens, A. P. Gray, F. J. Martens, and J. L. Boffey. 2008. Observations of avoidance reactions of migrating salmon to a mobile survey vessel in a riverine environment. Canadian Journal of Fisheries and Aquatic Sciences 65:2178–2190.